

Support for the Slope Sea as a major spawning ground for Atlantic bluefin tuna: evidence from larval abundance, growth rates, and particle-tracking simulations

Christina M. Hernández, David E. Richardson, Irina I. Rypina, Ke Chen, Katrin E. Marancik, Kathryn Shulzitski, and Joel K. Llopiz

Abstract: Atlantic bluefin tuna (*Thunnus thynnus*) are commercially and ecologically valuable, but management is complicated by their highly migratory lifestyle. Recent collections of bluefin tuna larvae in the Slope Sea off northeastern United States have opened questions about how this region contributes to population dynamics. We analyzed larvae collected in the Slope Sea and the Gulf of Mexico in 2016 to estimate larval abundance and growth rates and used a high-resolution regional ocean circulation model to estimate spawning locations and larval transport. We did not detect a regional difference in growth rates, but found that Slope Sea larvae were larger than Gulf of Mexico larvae prior to exogenous feeding. Slope Sea larvae generally backtracked to locations north of Cape Hatteras and would have been retained within the Slope Sea until the early juvenile stage. Overall, our results provide supporting evidence that the Slope Sea is a major spawning ground that is likely to be important for population dynamics. Further study of larvae and spawning adults in the region should be prioritized to support management decisions.

Résumé : Si le thon rouge de l'Atlantique (*Thunnus thynnus*) revêt une valeur commerciale et écologique, sa gestion est compliquée par son mode de vie hautement migratoire. Des prélèvements récents de larves de thon rouge dans la « Slope Sea » au large du nord-est des États-Unis ont soulevé des questions concernant la contribution de cette région à la dynamique de la population. Nous avons analysé des larves prélevées dans la Slope Sea et le golfe du Mexique en 2016 dans le but d'estimer l'abondance et les taux de croissance des larves et avons utilisé un modèle de circulation océanique régionale de haute résolution pour estimer les lieux de frai et le transport de larves. Nous n'avons relevé aucune différence régionale des taux de croissance, mais avons constaté que, avant le début de l'alimentation exogène, les larves de la Slope Sea étaient plus grandes que celles du golfe du Mexique. Les larves de la Slope Sea revenaient généralement à des lieux situés au nord du cap Hatteras et auraient été retenues dans la Slope Sea jusqu'au stade juvénile précoce. Globalement, nos résultats appuient l'interprétation voulant que la Slope Sea soit un lieu de frai majeur susceptible d'être important pour la dynamique de la population. Une priorité devrait être accordée à de nouvelles études des larves et des adultes reproducteurs dans la région pour appuyer la prise de décisions de gestion. [Traduit par la Rédaction]

Introduction

Atlantic bluefin tuna (*Thunnus thynnus*) are an iconic marine species — valuable to commercial and sport fishers alike and ecologically important for their role as top predators. However, their highly migratory life cycle complicates the study and management of their populations because individuals routinely cross international boundaries and utilize different areas of the ocean on both short (annual) and long (life-span) time scales (Mather et al. 1995). Tagging studies (Block et al. 2005; Galuardi and Lutcavage 2012; Block et al. 2001), otolith microchemistry (Rooker et al. 2008; Rooker et al. 2014), and population movement models (Kerr et al. 2013) have advanced our understanding of adult movements and stock structure. Still, there are outstanding questions about the distribution of spawning and larval habitat that can affect our life cycle models and, as a result, resource management decisions.

Although the prevailing understanding is that Atlantic bluefin tuna (bluefin hereinafter) comprise two populations with strong natal homing to spawning grounds in the Gulf of Mexico and the Mediterranean Sea, there has long been speculation that spawning may occur in other regions (Mather et al. 1995; Lutcavage et al. 1999). Evidence from tagging in the western Atlantic has shown that large individuals (presumed mature) may not visit either the Gulf of Mexico or the Mediterranean during the spawning season (Galuardi et al. 2010; Block et al. 2005). Studies of gonad status have also suggested that some western bluefin spawn much closer to the Gulf of Maine feeding grounds than in the Gulf of Mexico (Baglin 1976; Goldstein et al. 2007). Furthermore, although very few bluefin under 210 cm fork length (FL) are observed in the Gulf of Mexico (Richardson et al. 2016a; Diaz and Turner 2007), reproductive hormones indicate that individuals as small as 134 cm FL are reproductively capable (Heinisch et al. 2015).

Received 21 December 2020. Accepted 11 October 2021.

C.M. Hernández* and J.K. Llopiz. Biology Department, Woods Hole Oceanographic Institution, Woods Hole, MA 02543, USA.

D.E. Richardson and K.E. Marancik. Northeast Fisheries Science Center, National Oceanic and Atmospheric Administration, Narragansett, RI 02882, USA.

I.I. Rypina and K. Chen. Physical Oceanography Department, Woods Hole Oceanographic Institution, Woods Hole, MA 02543, USA.

K. Shulzitski. Cooperative Institute for Marine and Atmospheric Studies, University of Miami, Miami, FL 33149, USA.

Corresponding author: Christina M. Hernández (email: cmh352@cornell.edu).

*Present address: Ecology and Evolutionary Biology Department, Cornell University, Ithaca, NY 14850, USA.

© 2021 The Author(s). This work is licensed under a [Creative Commons Attribution 4.0 International License](https://creativecommons.org/licenses/by/4.0/) (CC BY 4.0), which permits unrestricted use, distribution, and reproduction in any medium, provided the original author(s) and source are credited.

Larval surveys near Cuba, the Straits of Florida, and the Blake Plateau have all found some larval bluefin, but never in numbers or abundance high enough to compare with the Gulf of Mexico and Mediterranean spawning grounds (McGowan and Richards 1989; Lamkin et al. 2019).

In 2013, larval bluefin were collected during ecosystem sampling in the Slope Sea, a wedge of ocean bounded by the US shelf break and the Gulf Stream as it peels away from the US east coast, at abundances comparable to levels typically found during the annual larval bluefin surveys in the Gulf of Mexico (Richardson et al. 2016a). Together with past lines of evidence from tagging, histology, and reproductive hormones, an alternate hypothesis of bluefin life history was put forward: that both the eastern and western stocks exhibit maturity at 3–5 years of age, but that younger western bluefin spawn in the Slope Sea until they reach a size where the longer migration to the Gulf of Mexico is favorable (Richardson et al. 2016a). The younger bluefin that are hypothesized to occupy the Slope Sea during the spawning season were estimated, as a spawning class, to have a higher biomass than the older bluefin that occupy the Gulf of Mexico, which in combination with the larval abundances in the Slope Sea led to the classification of this region as a third major spawning ground (Richardson et al. 2016a, 2016b).

The response to this discovery has been mixed, with some voices expressing skepticism about the origin of larvae or asserting that classification as a spawning ground was premature (Walter et al. 2016; Safina 2016) and others arguing that it calls for more innovative studies to resolve our understanding of bluefin life history (Di Natale 2017). To assess the classification of the Slope Sea as a major spawning ground, it is necessary to obtain more years of larval sampling and to focus on estimates of larval abundance instead of catch per tow (Walter et al. 2016). Although the temperature and transport conditions in the Slope Sea are suitable for bluefin spawning, larval growth, and larval retention (Rypina et al. 2019, 2021), there are important open questions about whether conditions in the Slope Sea actually support larval bluefin growth and survival. Another argument against the assertions of Richardson et al. (2016a) is that drifter transit times were used to imply that larvae could not have originated in the Gulf of Mexico, but actual spawning locations were not estimated (i.e., via particle backtracking simulations). Additionally, evidence of Slope Sea spawning activity by adults has not been conclusively shown, partly because tagging has focused primarily on the largest individuals that routinely visit the Gulf of Mexico (Block et al. 2005). Tagging studies on the sizes that are most likely to use the Slope Sea for spawning (134–220 cm FL; Richardson et al. 2016a; Heinisch et al. 2015) and histological collections within the Slope Sea would help identify what proportion of adults in various size classes are reproductively active in the area. Finally, a major open question regards the implications of Slope Sea residency and spawning for population structure and mixing between the eastern and western stocks, which has prompted new studies of population genetics (Puncher et al. 2018; Rodríguez-Ezpeleta et al. 2019).

In this paper, we further evaluate the importance of the Slope Sea as spawning habitat for Atlantic bluefin and argue that larval observations from 2016 continue to support the classification of the Slope Sea as a third major spawning ground. We calculated the abundance of bluefin larvae from sampling on several cruises in the Slope Sea in the summer of 2016 as well as revisiting the 2013 observations to estimate abundance. Using otoliths from larvae collected in 2016 in both the Slope Sea and the Gulf of Mexico, we analyzed larval growth and compared larval growth in the two regions. Finally, we used a high-resolution ocean circulation model to estimate the locations of spawning activity that would have led to our larval observations in 2016 and to investigate

retention of larvae within the Slope Sea region until the onset of directed swimming.

Methods

Larval sampling methods

Larval samples from the Slope Sea were collected in 2016 during two cruises off the US northeast continental shelf, conducted by the Northeast Fisheries Science Center (NEFSC) of the National Oceanic and Atmospheric Administration (NOAA).

The first set of samples used in this study were collected during an approximately 72 h transit of the NOAA Ship *Gordon Gunter* from Rhode Island to Norfolk, Virginia, from 17 to 20 June 2016 (cruise ID GU1608). Plankton sampling was performed at 24 stations (63% of these occurred during the day) along the transit. Net tows employed a bongo net with 61-cm diameter openings and 333- μ m mesh, with an additional 20-cm bongo net with 165- μ m mesh mounted 0.5 m above the larger bongo, and a CTD (conductivity–temperature–depth sensor) mounted 1 m above the smaller one. To target the depths occupied by larval bluefin and billfish (Habtes et al. 2014; Reglero et al. 2018a) and minimize sampling time, the net was lowered to 25 m and brought back to the surface over a 5 min period, and this was repeated for a total tow duration of approximately 10 min. Tow locations were spaced evenly on transects crossing the north wall of the Gulf Stream to target a gradient of habitat characteristics. Specifically, using information from the 2013 collections of bluefin in the Slope Sea (Richardson et al. 2016a) and satellite-derived sea surface temperature data, sampling stations were chosen that crossed from colder waters, through waters presumed to be suitable for bluefin larvae, and into the Gulf Stream waters presumed to be less suitable. Samples from all 4 nets were preserved in 95% ethanol, which was refreshed after 24 hours.

The second set of samples were collected during the Atlantic Marine Assessment Program for Protected Species (AMAPPS) between 27 June and 25 August on the NOAA Ship *Henry B. Bigelow* (cruise ID HB1603). The primary objective of the AMAPPS survey was to evaluate the abundance and distribution of marine mammals, sea turtle and seabirds in the US Exclusive Economic Zone off northeastern United States (Northeast Fisheries Science Center and Southeast Fisheries Science Center 2016). Visual survey lines were broken into two strata. The first stratum has narrowly spaced lines from the 100 m isobath across the shelf break to the Slope Sea. The second stratum is further offshore and over deeper water with the survey lines more widely spaced (refer to online Supplementary material, Fig. S1¹). The AMAPPS cruise collected plankton samples along the survey lines to provide an ecosystem context for the protected species sightings. Sampling locations were not predetermined, but rather were timed to minimize disruption to the continuous daytime visual surveys. In general, plankton tows were conducted to begin the day (approximately 0500 local time), at lunchtime (approximately 1200), and after visual surveys were completed for the day (approximately 1800). These standard samples were collected with a 61-cm bongo net with 333- μ m mesh, with a CTD mounted on the wire 1 m above the bongo. The bongo was deployed to 200 m or within 5 m of the bottom, in an oblique tow at outgoing wire speed of 50 m·min⁻¹ and incoming wire speed of 20 m·min⁻¹. One of the net samples was preserved in 95% ethanol to preserve otoliths and DNA of ichthyoplankton, and the other net sample was preserved in 5% formaldehyde and seawater to optimize the morphological identification of zooplankton. The ethanol-preserved sample was refreshed after 24–48 hours.

In addition to these standard daytime bongo samples, additional plankton sampling was carried out at night (36% of total number of bongos tows were performed at night) in areas where the bottom depth exceeded 1000 m. At these nighttime stations,

¹Supplementary data are available with the article at <https://doi.org/10.1139/cjfas-2020-0444>.

the standard 61-cm bongo was deployed according to the standard protocol described above for the daytime samples. An additional tow with a weighted 2 m × 1 m frame net with 333-µm mesh was used to increase catch of bluefin and other ichthyoplankton for aging and genetic analyses; deployments of this net were double-oblique tows to 25 m over a 10 min period. Samples from the frame net were preserved in 95% ethanol, and the ethanol was refreshed after 24–48 hours. Each of the 61-cm bongo and 2 m × 1 m frame nets were deployed with a General Oceanics flowmeter. However, we do not use the 2 m × 1 m frame nets in our abundance calculations because previous work indicates that catchability of tuna is different in these samples when compared to standard bongo tows (Habtes et al. 2014).

Laboratory processing of plankton samples

From nearly every bongo station on GU1608 and HB1603, one of the net samples was processed at the Morski Instytut Rybacki in Szczecin, Poland, following established protocols for both ichthyoplankton (Walsh et al. 2015) and zooplankton analyses (Kane 2007). For the ichthyoplankton analysis, all fish larvae, fish eggs and cephalopod paralarvae were removed and counted. Fish larvae were then identified to the lowest possible taxonomic category, and larval body length was measured with an ocular micrometer. Identification of scombrid larvae, including bluefin, were then verified at the Narragansett Laboratory of the Northeast Fisheries Science Center using criteria described in Richards and Potthoff (1974).

Among the samples not sent to Poland, samples likely to contain bluefin larvae were processed to make ethanol-preserved individuals available for otolith and genetic analyses. Stations that were most likely to contain bluefin larvae were identified as those with bottom depth exceeding 1000 m, sea-surface temperature (SST) exceeding 22 °C, and sea surface salinity of 34.5–36 PSU. Bongo samples matching these specifications were sorted under a light microscope to extract all ichthyoplankton. From these ichthyoplankton, bluefin were identified using morphological characters (Richards and Potthoff 1974), and species identification for 3 of these fish was confirmed using genetic markers. A lower number of larval bluefin was subjected to genetic identification in this study relative to Richardson et al. (2016a) to ensure that sufficient sample sizes ($N = 80$) were provided for population genetics studies.

We sorted 11 samples collected with the smaller bongo net (20-cm diameter with 165-µm mesh) to evaluate whether there was extrusion of small bluefin larvae from the 333-µm mesh in the 61-cm bongo. Information on the 3 small bongo samples that contained tuna larvae is provided in Supplementary Table S1¹. Some of the bluefin larvae identified from the 20-cm bongo samples were used for ageing, but they were not included in calculations of abundance.

Bluefin larvae from the Slope Sea that were processed in the US were photographed using either a Leica M205 microscope with a phototube or a Nikon SMZ-1500 microscope with a Nikon Ri-2 camera and imaging software. The scale for photographs was determined using a microscope calibration slide. Fish standard lengths were measured in ImageJ from the tip of the bottom jaw to the tip of the notocord for pre-flexion larvae or to the point of flexion in post-flexion larvae.

Larval distribution maps and larval abundance

For the Slope Sea collection, we generated a map of the estimated abundance of bluefin larvae from 61-cm bongo net tows (including tows to both 200 m and 25 m depth). This abundance is a point estimate at each sampling location and is a relative measure, since catchability of larval fishes can be affected by vessel speed, net configuration, and day–night cycles. When both nets of the bongo station were processed, we summed the number of larvae and the volume filtered from the two nets of the bongo. Abundance for each tow, expressed as number (n) per 10 m² is calculated as $a_i = 10 \times n_i/v_i \times h_i$, where n_i is the number of individuals collected, v_i is the volume filtered, and h_i is the range of depth

sampled (Irisson et al. 2010). We plot negative observations (abundance of 0 larvae per m²) only at bongo sampling locations deeper than 1000 m and between 17 June (when our sampling starts) and 15 August (two weeks after our last collected larval bluefin). There were two bongo sampling stations that meet these criteria that were not processed in Poland or the US, so those two stations are excluded from maps and calculations of larval abundance. The cutoffs of 17 June and 15 August cover all of the dates when larvae were observed in the Slope Sea in both 2016 (this paper) and 2013 (Richardson et al. 2016a). These dates are also consistent with expectations from temperature-based estimates of the timing of spawning and larval occurrence in the Slope Sea (Reglero et al. 2018b; Rypina et al. 2019). We follow the methods of previous work on the Slope Sea (Richardson et al. 2016a) and focus on depths greater than 1000 m because the northeastern US shelf is extensively sampled for plankton by NOAA and bluefin larvae have rarely been found there.

However, we recognize that because larval sampling has occurred in the Slope Sea in only a few years, the choice of which samples to include or exclude can impact the abundance estimates. If spawning occurs during a discrete time period with a single peak spawning time and exhibits a spatial pattern with decreased spawning activity with increasing distance from the center of the spawning region, averaging over a larger area or a longer time period will result in lower average larval abundance estimates. As such, we calculated mean larval abundance using a variety of configurations and report the duration of sampling and total area sampled for that configuration (Supplementary Table S2¹). In particular, we looked at the effects of only including stations at 1000 m or deeper, of including the GU1608 cruise that performed targeted sampling across the north wall of the Gulf Stream, and of varying the sampling dates included. The larval bluefin survey in the Gulf of Mexico typically samples from 20 April to 31 May, a duration of 42 days; in 2016, Gulf of Mexico sampling occurred between 30 April and 30 May, a period of 31 days. We also calculated the abundance in the Gulf of Mexico in 2016 and in the Slope Sea in 2013. In all of these cases, we restrict analyses to samples collected with 61-cm bongo frames with 333-µm nets.

Additionally, we utilized the AMAPPS survey design (Supplementary Fig. S1¹) to estimate stratified mean abundance for bluefin larvae collected during the AMAPPS cruises in 2016 and 2013, with multiple timing windows. The stratified means are calculated by using the spatial overlay tools in the R packages *sp* (version 1.4-2) and *rgdal* (version 1.5-23) to identify stations falling within each stratum. We used a Universal Transverse Mercator projection, with the WGS84 datum, zone 18, to calculate stratum areas. The stratified mean is the mean of values within each stratum, weighted by stratum area.

We also report the area covered by each sampling configuration. For stratified mean configurations, the area is the sum of the areas of the two strata. For all other configurations in the Slope Sea, we calculated the convex hull of sampling locations with a 28-km buffer (approximately 0.25° latitude–longitude) and estimated the area in a WGS84 projection, zone 18. To estimate the area covered by sampling in the Gulf of Mexico, we manually drew a 0.25° latitude–longitude buffer around the sampling grid (following Scott et al. 1993) and estimated the area in a WGS84 projection, zone 16.

Age and growth analyses

Larval otoliths display daily growth increments, with each increment corresponding to one day of growth since the onset of exogenous feeding (Brothers et al. 1976). From the identified larvae in the Slope Sea samples, 66 bluefin larvae were selected for otolith analyses across the range of stations and lengths sampled. Of those 66, 9 larvae had issues with preservation (desiccation of tissues or otolith dissolution) that prevented successful extraction of otoliths.

Otoliths were extracted from individual larvae with dissecting pins; both sagittae and lapillae were extracted and placed flat side down on a glass microscope slide in type B immersion oil. Otoliths were imaged with a Leica DM2500 compound microscope with an oil-immersion 100× objective lens; images were taken with a Leica MC120 HD camera and the Leica Application Suite software. Images were calibrated using a stage micrometer. Otoliths were read in ImageJ using the ObjectJ plug-in. All extractions and reads were performed by the same reader. For each larva, sagittae and lapillae were identified based on otolith radius, because the sagittae are larger. If two sagittae had been extracted, the clearest was selected for reading. There were 8 larvae for which we were able to extract and photograph only 1 or 2 otoliths. Among these 8, there were 3 fish from which we had extracted 2 otoliths with a visible size difference. This leaves 5 for which we could not use visual cues to determine if we had extracted a sagittal otolith (for 3 larvae, we extracted 1 otolith, and for another 2 larvae, we extracted 2 otoliths that did not have a visually obvious size difference). After reading otoliths from all larvae (see below), we analyzed how these 5 larvae were distributed on a plot of otolith radius vs. otolith increments (Supplementary Fig. S2¹). We found that 3 of the otoliths in question fell in the middle of the distributions of otolith radius, given the number of increments. The other 2 otoliths were the two smallest among otoliths with 2 daily increments. These 2 fish were excluded from the subsequent analyses.

The selected images of sagittal otoliths, one per larva, were read once, the order of the images was shuffled, and they were read again. If the two reads yielded ages within ± 1 day, the second read was retained. If the two reads differed by more than 1 day, a third read was performed. If the third read agreed to within ± 1 day of either the first or second read, then the third read was retained. If the third read differed by more than 1 day from both the first and second reads, then that fish was not retained in age analyses.

In addition to the Slope Sea samples, otoliths were analyzed from 143 larval bluefin collected in the Gulf of Mexico in 2016 by the Southeast Fisheries Science Center (SEFSC) as part of the Southeast Area Monitoring and Assessment Program (SEAMAP). These larvae were collected by oblique tows of a 61-cm bongo, either following the standard protocol with 333- μ m mesh to a sampling depth of 200 m, or with 505- μ m mesh to a sampling depth of 10 m. The 143 larvae that were examined were selected to cover a range of locations, oceanographic conditions, and sizes. For all of these larvae, standard length was also measured. The same protocols were used for extracting otoliths as for the Slope Sea larvae. Otoliths for Gulf of Mexico bluefin larvae were imaged with a Zeiss Axio Scope.A1 compound microscope with an oil-immersion 100× objective lens; images were taken with a Qimaging MicroPublisher 3.3 RTV camera and ImagePro Plus 7 software.

Both the Slope Sea and Gulf of Mexico otoliths from 2016 were read by the same reader following consistent protocols for marking images and quality control of reads. After quality control, 52 larval otoliths from the Slope Sea and 142 from the Gulf of Mexico were retained for age and growth analyses.

We used linear least-squares to fit age–length relationships for the Slope Sea and Gulf of Mexico data sets. Because the Slope Sea data set had no larvae with more than 8 increments, and few larvae with more than 4 increments, we also estimated best-fit lines for three subsets of the data: larvae from the Gulf of Mexico with 0–8 increments, larvae from the Gulf of Mexico with 0–4 increments, and larvae from the Slope Sea with 0–4 increments. The slopes of these lines are estimates of the daily growth rates for each of the data sets or subsets.

We used an analysis of covariance (ANCOVA) approach to determine if there is a significant effect of region on either the slope or intercept of the linear models of the age–length relationships. We pooled the data from the Gulf of Mexico and the Slope Sea,

and added a factor for region. We then used the aov function in R (version 4.0.2) to fit a linear model to these data, including an interaction term between the number of increments and the region. This function returns a *p* value for each covariate and the interaction term. If the interaction term was not significant, we interpreted this as no significant difference in the slopes of the two regression lines. We then used the aov function without the interaction term to test for a significant effect of region on the intercept of the best-fit lines. We performed this step-wise analysis for all larvae with 0–8 increments and then a second time for the subset of larvae with 0–4 increments.

Otolith radius tends to be strongly correlated with larval length, so the width of each daily increment is a proxy for daily growth rate, and the distance (or radius) to each daily increment is a proxy for length at age (Sponaugle et al. 2009). We measured the increment width for increments within a given otolith starting from the first daily growth ring (e.g., a larva with 5 increments marked will yield 4 increment widths, corresponding to 4 days of larval growth). To control for effects such as selective mortality, we restricted our analysis of Gulf of Mexico increment widths and otolith radii to only those larvae with 8 or fewer increments, since the oldest larva in our Slope Sea data set has 8 increments. For each regional data set, we calculated the mean increment width and mean radius to increment for each day of larval life if there are at least 3 larvae with that increment (i.e., we did not calculate a mean increment width for the Slope Sea for increments 6 or 7 because there are only 2 larvae with 7 rings and 1 larva with 8 rings). We also calculated the standard error of the mean as σ/\sqrt{n} , where σ is the sample standard deviation and *n* is the sample size at that increment index.

We also tested for a significant difference in the mean otolith radius at the first increment between the Slope Sea and the Gulf of Mexico, using a two-sided Welch *t* test. We performed this test for larvae with 0–8 increments and then again for those larvae with 0–4 increments.

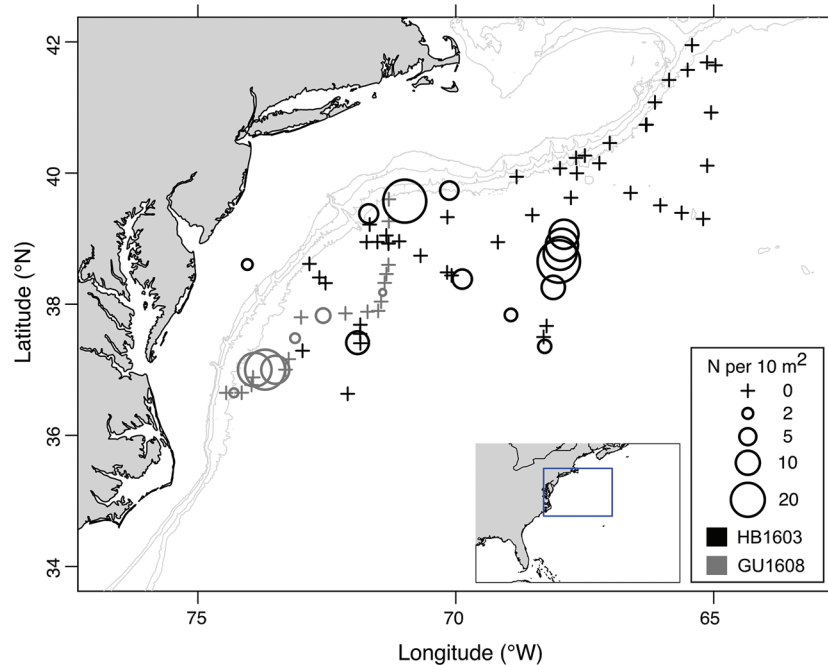
Larval drift simulations

We estimated the spawning locations and larval transport trajectories of larvae collected in the Slope Sea in 2016 using particle backtracking in a regional ocean circulation model (MABGOM2). The same model was used in Rypina et al. (2019). This regional ROMS-based model is specifically constructed for the continental shelf and slope region off northeastern US and has a high resolution of 1 km in the cross-shore direction and 2 km in the along-shore direction. The MABGOM2 model was previously validated for the Slope Sea region based on in situ hydrographic observations and satellite altimetry data for 2013 (Rypina et al. 2019). The configuration of the MABGOM2 model for 2016, which is used here, is identical to that for the 2013 MABGOM2 model run. More details about MABGOM2 can be found in Rypina et al. (2019).

As this high-resolution model is capable of resolving the realistic circulation features of interest at both meso- and submeso-scale, we treat the larval trajectories as deterministic and do not add any stochasticity to the simulated larval drift. (Note that the addition of a small stochastic component appropriate for representing the un- and under-resolved scales of motion does not significantly change our results due to the short duration of larval trajectory integration: ≤ 27 days). We use model velocity fields at 10 m below the ocean surface to advect simulated larvae (Habtes et al. 2014; Reglero et al. 2018a). Larval trajectory back- and forward-tracking is performed using the fourth-order variable-step Runge–Kutta scheme (built-in function “ode45” in Matlab) with a bi-linear interpolation between velocity grid points in both time and space; identical integration and interpolation numerical schemes were used in Rypina et al. (2014, 2016, 2019).

Larvae included in otolith analyses had direct age estimates available for use in backtracking simulations. For larvae that were not aged, we used the overall size-at-age relationship derived

Fig. 1. Abundance of Atlantic bluefin tuna larvae in the Slope Sea in 2016. Abundance of Atlantic bluefin tuna (*Thunnus thynnus*) larvae, expressed as number (n) per 10 m^2 . Data are shown for all bongo stations at locations with 1000 m depth or greater that were sampled between 17 June and 15 August, plus one station on the shelf where bluefin larvae were observed. Sampling stations are separated by cruise, with the marine mammal survey cruise (HB1603) shown in black and the earlier Gulf Stream crossing sampling cruise (GU1608) shown in dark grey. Bathymetric contours at 100, 200, 1000, and 2000 m depth are shown in light grey (accessed through GEBCO). Coastlines are the coastlineWorldFine data from the ocedata package in R, and the aspect ratio for plotting is automatically chosen by R for the latitude and longitude at the center of the plot.



from Slope Sea otolith analyses to estimate the number of daily growth increments. We also accounted for spread around the best-fit line by defining the distribution of expected ages using the best-fit line as the mean and the standard deviation of the residuals as the variance. For each larva that was measured but not aged, we drew a value from this normal distribution and then rounded it to the nearest 1 day, resulting in an estimated number of increments for that larva. There were 3 larvae with missing length data — we assumed the length of these larvae to be the average length of all measured bluefin larvae collected at that station.

This gives age in days since the onset of exogenous feeding, but to inform backtracking, we needed estimated ages in days post-spawning. At the typical temperatures of field collections of larval bluefin in the Slope Sea, it takes 30–50 hours for bluefin eggs to hatch (Reglero et al. 2018b) and approximately 2 days until the onset of exogenous feeding after hatching (Yúfera et al. 2014). Therefore, we added 4 days to convert the estimates of increment number into age of each larva in days post-spawning, which is also consistent with work on Pacific bluefin tuna (*Thunnus orientalis*) reared in the laboratory (Itoh et al. 2000). We performed individual-based particle simulations for each unique combination of station and larval days post-spawning. These simulations were run backwards in time to the estimated spawning date.

Additionally, we ran simulations forward in time to examine whether the observed bluefin larvae would have been retained in the Slope Sea during the period of drift as eggs and larvae. Laboratory work on Pacific bluefin tuna indicates that they begin schooling at 25 days post-hatch (Fukuda et al. 2010). Therefore, we assume that bluefin are capable of directed swimming at 27 days post-spawning (2 days of egg duration plus 25 days post-hatch) and that the egg-and-larval drift period covers 27 days post-spawning. For each larva, we know their estimated age in days post-spawning and collection location — with this, we simulate

their trajectory forward in time until their age would have been 27 days post-spawning.

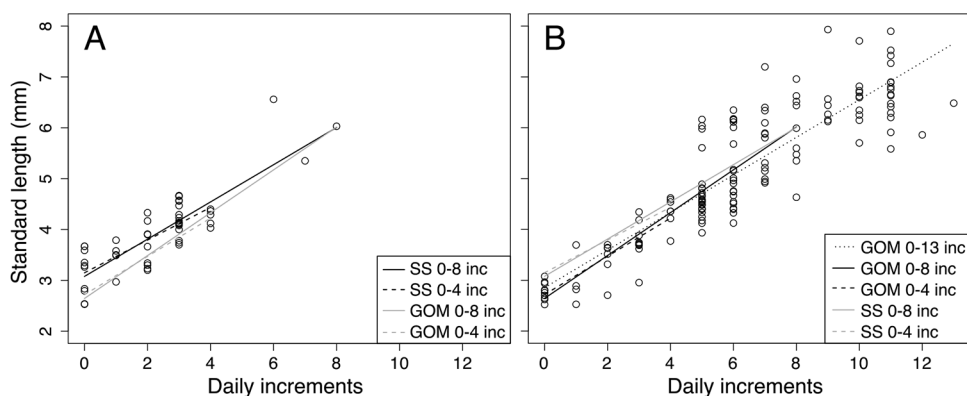
Results

In 2016, larval sampling in the Slope Sea yielded 225 bluefin larvae, ranging in size from 2 to 8.2 mm. Atlantic bluefin larvae were observed across a wide geographic area, from 36.65°N to 39.73°N and from 67.9°W to 74.3°W (Fig. 1; Supplementary Table S1¹). There was one bluefin larva collected at a station inshore of the shelf break, with a bottom depth of 55 m. All other observations of bluefin larvae were at locations with a bottom depth of 2000 m or greater. All but 7 of the bluefin larvae observed in the Slope Sea in 2016 were collected between 18 June and 13 July. Six bluefin larvae were collected on 31 July, and one additional bluefin larva was collected on 1 August — these two stations were also the northernmost observations.

At stations where bluefin larvae were observed, the abundance ranged from 0.80 to 31.75 bluefin larvae per 10 m^2 (mean = 11.29 larvae per 10 m^2 ; Supplementary Table S1¹). The highest abundance was observed on 31 July on the northeastern edge of the Mid-Atlantic Bight (Fig. 1). The second-highest abundance (31 larvae per 10 m^2) occurred within a cluster of high-abundance stations in the eastern portion of the sampling area on 8 July. The third-highest abundance (27.47 larvae per 10 m^2), along with two other high-abundance stations, was observed in the southwestern portion of the Slope Sea on 19–20 June.

The mean abundance of bluefin larvae across the Slope Sea in 2016 varied between 1.94 and 3.19 larvae per 10 m^2 , depending on the configuration of stations included (Supplementary Table S2¹). The highest estimate is attained when the sampling period is restricted to the AMAPPS cruise, stations 1000 m and deeper, and a time period of 42 days (to match the duration of typical sampling

Fig. 2. Larval growth curves for bluefin tuna larvae in 2016. Larval size-at-age for Atlantic bluefin tuna larvae (*Thunnus thynnus*) collected in (A) the Slope Sea and (B) the Gulf of Mexico in 2016. On each plot, circles show the standard length (mm) for larvae with 0–13 daily growth increments. The black lines are best-fit lines to the circles, and the grey lines show the best-fit lines from the opposite panel. Solid lines show the relationship for larvae with 0–8 increments, dashed lines correspond to larvae with 0–4 increments, and the dotted line in panel B shows the best-fit line for the overall data set from the Gulf of Mexico (0–13 increments).



in the Gulf of Mexico); this set of samples covers an area of 262 471 km². The mean abundance for the configuration of samples included in Fig. 1 (both cruises, 17 June – 15 August, stations at 1000 m or deeper) is 2.80 larvae per 10 m², over an area of 283 959 km². When we drop the mid-June sampling that used shallower bongo tows on a transect across the north wall of the Gulf Stream (the GU1608 samples) and include only the AMAPPS cruise between 28 June and 15 August (49 days) at 1000 m or deeper, the mean abundance is estimated to be 2.79 larvae per 10 m² over an area of 262 471 km². The stratified mean, which takes into account the AMAPPS cruise design, provides a similar estimate (2.55 or 2.46 larvae per 10 m²) for a duration matching either typical SEAMAP sampling (42 days) or the SEAMAP duration in 2016 (31 days). The combined area of the two strata is 308 704 km².

In the Gulf of Mexico in 2016, station abundance ranged from 3.95 to 356.83 larvae per 10 m² (Supplementary Fig. S3¹). The estimated mean abundance in the Gulf of Mexico, using the full SEAMAP survey from 2016 (31 days), is 12 larvae per 10 m² over an area of 447 676 km².

We also calculated station abundances for the bongo stations where bluefin larvae were observed in the Slope Sea in 2013 (Richardson et al. 2016a) and found that they ranged from 2.58 to 116.9 bluefin per 10 m², with an average of 28.59 bluefin per 10 m² among the 8 positive bongo stations. Estimates of larval abundance for the Slope Sea in 2013 range from 1.24 to 5.23 larvae per 10 m², depending on the configuration. The stratified mean abundance for the full AMAPPS cruise in 2013 (48 days) is 2.66 larvae per 10 m².

Larvae from the Slope Sea that were used in otolith analyses ranged from 2.53 to 6.56 mm and had 0 to 8 increments (Fig. 2A). The 52 larvae with high-quality otolith data represent a wide geographic range of observations, although no larvae were aged from several of the low-abundance stations in the central region of the sampling area (Supplementary Fig. S4A¹). The larvae we aged were collected between 19 June and 12 July (Supplementary Table S1¹).

The estimated growth rate for bluefin larvae collected in the Slope Sea was 0.37 mm·day⁻¹, and the estimated length at 0 increments was 3.08 mm (Fig. 2A). However, there are few larvae with more than 5 increments. If we restricted our analysis to only those larvae with 4 or fewer increments, we found that the estimated growth rate was slightly lower (0.32 mm·day⁻¹), and the estimated length at 0 increments was slightly higher (3.15 mm).

Larvae from the Gulf of Mexico that were used in otolith analyses ranged from 2.52 to 7.93 mm and from 0 to 13 increments. The

142 larvae with high-quality otolith data represent a wide geographic range of sampling locations across the northern Gulf of Mexico (Supplementary Fig. S4B¹). These larvae were collected between 30 April and 30 May 2016.

The estimated growth rate for bluefin larvae collected in the Gulf of Mexico in 2016 was 0.37 mm·day⁻¹, and the estimated length at 0 increments was 2.85 mm (Fig. 2B). If we restricted our analysis to only those larvae with 8 or fewer increments (to facilitate comparison with the Slope Sea data), we found that the estimated growth rate was 0.42 mm·day⁻¹, and the estimated length at 0 increments was 2.65 mm. If we restricted our analysis to only those larvae with 4 increments or fewer (again, for comparison with the Slope Sea data), we found that the estimated growth rate was 0.38 mm·day⁻¹, and the estimated length at 0 increments was 2.72 mm.

The stepwise ANCOVA analysis found no significant effect of region (Slope Sea vs. Gulf of Mexico) on the slope of the larval age–length relationship in our data set ($p = 0.24$ for 0–8 increments, $p = 0.31$ for 0–4 increments). There was, however, a significant effect of region on the intercept ($p < 0.01$ for 0–8 increments, $p < 0.0001$ for 0–4 increments). Therefore, we determined that there is no significant difference in the average daily growth rate of bluefin larvae based on whether they were collected in the Slope Sea or the Gulf of Mexico, but that the larvae collected in the Slope Sea were significantly larger prior to exogenous feeding and potentially at hatching.

In our measure of daily growth rate, using increment width as a proxy for daily growth, we observed that the first 3 increment widths (from increments 1 through 3 to increments 2 through 4) are extremely similar in the Slope Sea and the Gulf of Mexico (Fig. 3A). The error bars for Slope Sea values at increments 4 and 5 also overlapped with Gulf of Mexico values, but the small sample size of Slope Sea larvae over 4 increments restricted our ability to interpret those values. Otolith radius, as a proxy for larval size, is higher in Slope Sea larvae at the first increment, and then that difference appears to carry over across the rest of the increments (Fig. 3B).

The average distance to the first otolith increment is higher in the Slope Sea (12.21 μm for larvae with 0–8 increments and 12.16 μm for larvae with 0–4 increments) than in the Gulf of Mexico (11.29 μm for larvae with 0–8 increments and 11.58 μm for larvae with 0–4 increments). The Welch t test determined that this difference was statistically significant for the larvae with 0–8 increments ($p < 0.0001$) and for larvae with 0–4 increments ($p = 0.029$).

Fig. 3. Otolith measurements from bluefin tuna larvae collected in 2016. Otolith increment width is a proxy for daily growth rate on a given day of larval growth (e.g., width of increment 1 is measured as the distance between the first and the second increments), and otolith radius to a given increment is a proxy for larval size. To compare between the Slope Sea and Gulf of Mexico data sets, we include only those larvae with 0–8 increments. For each region, the mean increment width (A) and the mean radius to increment (B) are shown for each day of larval life if there are at least 3 larvae with that increment. Error bars show the standard error of the mean, calculated as σ/\sqrt{n} , where σ is the sample standard deviation and n is the sample size at that increment index.

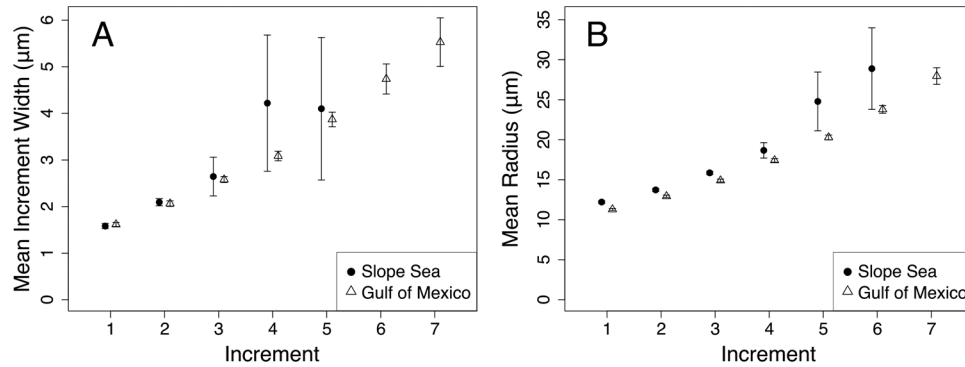
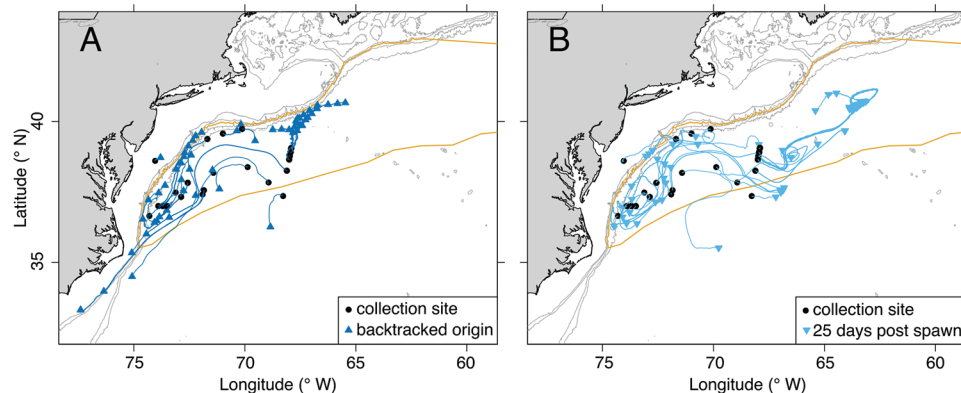


Fig. 4. Simulated trajectories for larvae collected in the Slope Sea in 2016. For each unique combination of station and age (days post-spawning, either estimated directly from otoliths or indirectly from the age–length relationship), larval trajectories were simulated backwards in time to estimate spawning location (A) and forwards in time until the onset of directed swimming behavior (an estimated larval age of 27 days post-spawning; B). Bathymetric contours at 100, 200, 1000, and 2000 m depth are shown in light grey (accessed through GEBCO). The Slope Sea bounding box (orange outline) is defined in Richardson et al. (2016a); the shapefile, which uses a WGS84 projection, was downloaded from <https://marineregions.org/gazetteer.php?p=details&id=59314>. Coastlines are the coastlineWorldFine data from the ocedata package in R, and the aspect ratio for plotting is automatically chosen by R for the latitude and longitude at the center of the plot. [Colour online.]



Particle tracking simulations for Slope Sea larvae placed the vast majority of larvae within the Slope Sea domain on the estimated day of spawning and at the onset of directed swimming (approximately 25 days post-hatch, (Fukuda et al. 2010) or 27 days post-spawning). We observed 60 unique combinations of collection location and estimated age in days post-spawning in the Slope Sea in 2016. There were 53 trajectories, representing 217 larvae, that backtracked to locations within the Slope Sea, which formed 3 clusters near (1) the southeastern flank of Georges Bank, (2) the shelf slope off New Jersey and Maryland, and (3) the southwestern corner of the Slope Sea (Fig. 4). There were 5 trajectories, representing 6 larvae, that backtracked to locations outside of the southern boundary of the Slope Sea near Cape Hatteras. There was one bluefin larva collected on the shelf that was estimated to have been spawned on the shelf, as well as 1 larva that was collected outside of the Slope Sea in the Gulf Stream region that backtracked to that same area near 35°N, 65°W (Fig. 4). There were 53 simulated trajectories, representing 217 larvae, that were retained within the Slope Sea until 27 days post-spawning, and 7 trajectories, representing 8 larvae, that exited the MABGOM2 model domain through the

eastern boundary — and 4 of these are trajectories that also backtracked to locations near Cape Hatteras (Fig. 4 and Supplementary Fig. S5¹). The 6 sampling locations that correspond to larvae that were not retained in the Slope Sea (or the MABGOM2 model domain) until 27 days post-spawning all correspond to locations along the Gulf Stream boundary of the Slope Sea (Supplementary Fig. S5¹).

Discussion

The collections of Atlantic bluefin larvae in the Slope Sea in 2016, together with the otolith analyses and particle tracking simulations that they enabled, support the conclusion that the conditions in the Slope Sea are suitable for their growth and retention and that they originated from spawning within the Slope Sea. Larvae were observed across a wide geographic area in the Slope Sea from mid-June to early August, with a mean abundance of approximately 2.5 larvae per 10 m². Otolith analyses found that in 2016, Slope Sea larvae appear to have hatched at larger sizes and grew at similar rates to larvae collected in the Gulf of Mexico. Particle backtracking simulations confirmed that larvae collected in the Slope Sea were spawned in the Slope Sea.

These results support the previous assertions that widespread spawning by bluefin occurs in the Slope Sea and that the conditions are suitable for spawning and larval growth (Richardson et al. 2016a; Rypina et al. 2019).

At the broadest and simplest scale of comparison, the temporal and spatial extent of larval observations in the Slope Sea are consistent with a broad region of spawning habitat. In our study as well as previous larval studies in the Slope Sea, Gulf of Mexico, and Mediterranean, larval observations generally span a 2-month period, with the phenology modulated by local environmental conditions (Richardson et al. 2016a; Reglero et al. 2018b). The locations of larval presence in the Slope Sea in 2016 spanned 8° of longitude and 4° of latitude (Fig. 1); larvae were observed across 12° of longitude and 5° of latitude during 25 years of comprehensive sampling in the Gulf of Mexico (Muhling et al. 2010). In the Mediterranean, spawning occurs across an even larger spatial extent, but much of the recent sampling focus has been on the smaller spawning hotspot around the Balearic Islands, an area of 5° longitude by 2° latitude (Alemany et al. 2010). Although a degree of longitude is not equidistant at all latitudes, our larval observations and estimated spawning locations are widespread in the Slope Sea, and this is consistent with the results of Rypina et al. (2019) and Rypina et al. (2021) that suitable spawning habitat is amply available in this region.

Observations of larval bluefin abundance in the Slope Sea are comparable to those from the Gulf of Mexico and the Mediterranean given the limited sampling in the Slope Sea and the highly patchy nature of bluefin larvae. The overall mean abundance of bluefin larvae at sampling stations around the Balearic Islands in the Mediterranean from 2001 to 2005 was 4.3 larvae per 10 m² (Alemany et al. 2010), nearly twice as high as our estimate from the Slope Sea. We estimated that the mean larval abundance in the Slope Sea in 2016 and 2013 was approximately 2.5 larvae per 10 m² and that the mean abundance in the Gulf of Mexico in 2016 was 12 larvae per 10 m² (Supplementary Fig. S3¹). The estimate for the Gulf of Mexico in 2016 is nearly 5 times as high as our estimate for the Slope Sea (and nearly 3 times as high as the estimate from the Mediterranean), but it is important to point out that the larval abundance index in the Gulf of Mexico in 2016 is 4.5 times higher than its average from the preceding decade (Ingram 2018; ICCAT 2019).

There are few peer-reviewed publications on the time series of larval bluefin abundance in the Gulf of Mexico, since studies of larval bluefin report an abundance time series that combines multiple tuna taxa (Lindo-Atichati et al. 2012; Domingues et al. 2016; Habtes et al. 2014) or focus on probability of occurrence (Muhling et al. 2010, 2013; Domingues et al. 2016). One time series that is available is the larval abundance index, which uses statistical fitting methods related to the timing and seasonality of larval collections, as well as the swept area of sampling and the estimated ages and mortality rates of larvae to estimate the average number of larvae per 100 m² at first daily otolith increment formation, across the Gulf of Mexico sampling domain (Ingram et al. 2010; Ingram 2018). The mean larval abundance index from 1981–2015 is 0.50, while the value in 2016 was 2.46, nearly 5 times the mean in the preceding 35 years (see “ZIDL” in table 4 of Ingram 2018). Although a direct comparison is difficult, it would appear that the larval abundance estimates from the Slope Sea are consistent with observations in the Gulf of Mexico between 1981 and 2015.

The scope of larval bluefin collections in the Slope Sea in 2016 — 207 larvae collected at 20 out of 79 bongo stations — align much better with collections from the major spawning grounds than with other scattered observations. For example, the Slope Sea larvae are often compared with a southeastern US cruise that found 14 larvae at 10 stations out of 147 sampled stations (McGowan and Richards 1989), the surveys in Mexican waters near Campeche Bank that found 5 larvae at 4 stations out of

sampling at 40 stations (Muhling et al. 2011), or the survey north and east of the Bahamas that found 18 larvae at 9 out of 97 stations using a net and tow protocol designed to optimize the collection of bluefin larvae (Lamkin et al. 2014). That is a 7% positive station rate in the southeastern US region, a 10% positive rate in Mexican waters, and a 9% positive rate near the Bahamas. We estimate a 25% positive station rate in the Slope Sea in 2016, which agrees well with the SEAMAP positive station rate of 0%–30% (mean of 15%) between 1993 and 2009 (Domingues et al. 2016) and a 14% positive station rate in the Balearic Sea surveys from 2001 to 2005 (Alemany et al. 2010). By several metrics, the distribution of bluefin larvae in the Slope Sea is comparable to the observations on the two other recognized major spawning grounds.

Our growth analyses, performed with the same reader analyzing otoliths from both the Slope Sea and the Gulf of Mexico from 2016, reveal that Slope Sea larvae grew at comparable rates to Gulf of Mexico larvae. Otolith analyses from bluefin larvae collected in the Balearic Sea in 2003–2005 estimated the growth rate at 0.35 to 0.41 mm·day⁻¹ (García et al. 2013), similar to the rates that we estimated for both the Slope Sea and Gulf of Mexico in 2016 (Fig. 2). Another study of larval bluefin growth analyzed larvae collected in the Gulf of Mexico in 2000–2012 and found a lower intercept (2.24 vs. 2.85 mm) and higher slope (0.46 vs. 0.37 mm·day⁻¹) as compared to our results from the Gulf of Mexico in 2016, for a similar size and age range of larvae (Malca et al. 2017). Data from an older study of bluefin larvae collected in the Straits of Florida (Brothers et al. 1983) provides a lower estimate of larval growth, approximately 0.27 mm·day⁻¹ (McGowan and Richards 1989). There may be interannual variability in larval growth conditions on the various spawning grounds, as has been shown in the Balearic Sea (García et al. 2013), but detailed studies of interannual variability in larval growth have not been published for the Gulf of Mexico. A single year of comparison is insufficient; if growth conditions in the Gulf of Mexico were anomalously poor in 2016 (for example, due to the high larval abundance that was observed), then our comparison of Slope Sea and Gulf of Mexico growth rates is incomplete. While the samples exist to enable a study of interannual variability in larval bluefin growth in the Gulf of Mexico, we need several more years of sampling in the Slope Sea to be able to characterize the interannual variability in larval growth there.

Our otolith analyses also suggest that Slope Sea larvae were larger at the onset of exogenous feeding in 2016, using two different proxies. The intercept of the size-at-age relationship (Fig. 2) and the otolith radius to the first increment (Fig. 3B) were both found to be significantly higher in the Slope Sea than in the Gulf of Mexico, regardless of whether we used a data set including larvae with 0–8 increments or 0–4 increments. There are two possible mechanisms for a difference in larval size at hatching: temperature and maternal provisioning. Larval length at hatching for a given species decreases with increasing temperature (Peck et al. 2012). The average SST at the time of collection for aged larvae from 2016 from the Slope Sea was 25.5 °C, and it was 27.0 °C for aged larvae from the Gulf of Mexico. This temperature difference may be sufficient to account for the difference in size at hatching. On the other hand, larval size at hatching and growth before the onset of exogenous feeding also depend on the resources provided in the egg, which has been shown to be related to body condition of the mother (Chambers et al. 1989). The maternal condition and allocation of resources (both per-egg provisioning and total provisioning) to reproduction depend on size, recent food availability, and metabolic activity (Green 2008). Increased maternal provisioning in Slope Sea larvae could indicate that Slope Sea spawning adults are able to allocate more resources to reproductive activity than are Gulf of Mexico spawning adults; this could be due to the shorter spawning migration distance to the Slope Sea (Chapman et al. 2011). However, reproductive investment and offspring quality can also vary with maternal size or age (Green 2008),

so it is important that we identify the distribution of ages among bluefin that spawn in the Slope Sea.

Although it was previously estimated that none of the larvae collected in the Slope Sea in 2013 could have been spawned in the Gulf of Mexico or the Straits of Florida (Richardson et al. 2016a), the perception remains that larvae collected in the Slope Sea could easily be transported there from more southerly locations (Safina 2016) where small collections of larvae have been observed previously, such as the Straits of Florida (Brothers et al. 1983) and the Blake Plateau (McGowan and Richards 1989). In this study, we simulate larval trajectories using a high-resolution circulation model for the Mid-Atlantic Bight and Gulf of Maine (MABGOM2), which was previously validated using hydrocast data from NOAA cruises (Rypina et al. 2019). We find that nearly all (96%) of the larvae collected in the Slope Sea in 2016 backtrack to locations north of Cape Hatteras on the estimated dates of spawning (Fig. 4). When we simulated trajectories forward in time, we likewise found that nearly all (96%) larvae collected in the Slope Sea would have been retained within the Slope Sea domain (Fig. 4). For both backward and forward tracking, the handful of trajectories that originate or terminate outside of the Slope Sea correspond to larvae that were collected along the Gulf Stream front (Supplementary Fig. S5¹).

Previous work has used particle tracking simulations with larval growth and retention criteria to understand the distribution of suitable bluefin spawning habitat in the Slope Sea (Rypina et al. 2019) and the interannual variability of that suitable habitat (Rypina et al. 2021). These simulations have identified a persistent region of high spawning habitat suitability in the Mid-Atlantic Bight and the associated Slope Gyre (Rypina et al. 2021). The larval observations in both 2013 and 2016 were concentrated in these regions (Fig. 1; Rypina et al. 2019; Richardson et al. 2016a), as were our estimated spawning sites in 2016 (Fig. 4A). Taken together, this is strong evidence that repeated and predictable spawning activity by bluefin is possible in the Slope Sea.

It is imperative that we increase our studies of the Slope Sea to understand how bluefin spawning in this region influences the ecology and population dynamics of this valuable stock. Ichthyoplankton sampling occurs routinely on the northeastern US shelf (Walsh et al. 2015), but plankton monitoring, and ship traffic in general, is limited beyond the shelf break. However, the spatial and temporal patterns of larval tuna distributions in the Slope Sea are reliable and can be used to inform future cruises (Fig. 1; Rypina et al. 2019, 2021; Richardson et al. 2016a). Additional years of larval bluefin collections will strengthen our understanding of age and growth and enable us to build a time series of the larval abundance index in the Slope Sea (Scott et al. 1993; Ingram et al. 2010). With multiple years of data, we can investigate interannual differences and test for relationships between metrics of growth and environmental conditions. There is a need for ecological work on the diets and zooplankton food availability for bluefin larvae in the Slope Sea and comparisons with the other major spawning grounds (Llopiz and Hobday 2015).

An important open question is the abundance, distribution, and identity of the spawning adults in the Slope Sea. How many adults are spawning there, and do they consistently utilize the suitable habitat identified in Rypina et al. (2021)? Are they western individuals that mature earlier than previously understood, or is there significant stock mixing occurring between eastern and western individuals? Bluefin in the Slope Sea should be sampled across a wide range of sizes for histological analyses to determine what sizes of bluefin are reproductively active in the region. Reproductively active individuals can also be tested for stock identity using otolith microchemistry (Rooper et al. 2008) or population genetics (Puncher et al. 2018; Rodríguez-Ezpeleta et al. 2019).

Atlantic bluefin are an iconic commercial and sport fish that captivate human imaginations and taste buds. Climate change is threatening their ability to reproduce in the Gulf of Mexico, even

if they were to shift their phenology (Muhling et al. 2015). Spawning in the Slope Sea may offer the species additional resilience in the face of both harvesting and climate change. If we hope to conserve this species and sustain the industries that depend on it, we must acknowledge Slope Sea spawning and integrate it into our understanding of the bluefin life cycle and our management of stock dynamics.

Competing interests

The authors declare there are no competing interests.

Funding statement

Ship time was supported by NOAA, the Bureau of Ocean Energy Management, and the US Navy through interagency agreements for Atlantic Marine Assessment Program for Protected Species (AMAPPS). CMH and JKL received funding from the Woods Hole Oceanographic Institution's Ocean Life Institute (#13080700) and Academic Programs Office. CMH was additionally supported by the Adelaide and Charles Link Foundation and the J. Seward Johnson Endowment in support of the Woods Hole Oceanographic Institution's Marine Policy Center. IIR, KC, and JKL were supported by a US National Science Foundation (NSF) grant (OCE-1558806). JKL was additionally supported by the Lenfest Fund for Early Career Scientists and the Early Career Scientist Fund at Woods Hole Oceanographic Institution.

Author contributions

CMH, DER, and JKL conceived the project. CMH, DER, and KEM performed laboratory analyses on Slope Sea samples. KS provided Gulf of Mexico otolith images. IR and KC performed model simulations. CMH read all otoliths, analyzed data, prepared figures, and drafted the manuscript. All authors edited the manuscript.

Data availability statement

Data and code associated with this project are available on GitHub at <https://github.com/chris3815/SlopeSeaBluefinTuna>. All data collected by the CTD have been uploaded to the National Oceanographic Data Center (<https://www.nodc.noaa.gov/>).

Acknowledgements

The authors thank the crew and scientific parties of NOAA cruises HB1603, GU1608, and the 2016 SEAMAP cruises, as well as Glenn Zapfe for providing SEAMAP data.

References

- Aleman, F., Quintanilla, L., Velez-Belchí, P., García, A., Cortés, D., Rodríguez, J.M., et al. 2010. Characterization of the spawning habitat of Atlantic bluefin tuna and related species in the Balearic Sea (western Mediterranean). *Prog. Oceanogr.* 86(1–2): 21–38. doi:10.1016/j.pocan.2010.04.014.
- Baglin, R.E. 1976. A preliminary study of the gonadal development and fecundity of the western Atlantic bluefin tuna. *Collect. Vol. Sci. Pap. ICCAT*, 5: 279–289.
- Block, B.A., Dewar, H., Blackwell, S.B., Williams, T.D., Prince, E.D., Farwell, C.J., et al. 2001. Migratory movements, depth preferences, and thermal biology of Atlantic bluefin tuna. *Science*, 293(5533): 1310–1314. doi:10.1126/science.1061197. PMID:11509729.
- Block, B.A., Teo, S.L.H., Walli, A., Boustany, A., Stokesbury, M.J.W., Farwell, C.J., et al. 2005. Electronic tagging and population structure of Atlantic bluefin tuna. *Nature*, 434(7037): 1121–1127. doi:10.1038/nature03463. PMID:15858572.
- Brothers, E.B., Mathews, C.P., and Lasker, R. 1976. Daily growth increments in otoliths from larval and adult fishes. *Fish. Bull.* 74(1): 1–8. doi:10.1006/jfbi.1993.1006.
- Brothers, E.B., Williams, D., and Sale, P.F. 1983. Length of larval life in twelve families of fishes at "One Tree Lagoon", Great Barrier Reef, Australia. *Mar. Biol.* 76: 319–324. doi:10.1007/BF00393035.
- Chambers, R.C., Leggett, W.C., and Brown, J.A. 1989. Egg size, female effects, and the correlations between early life history traits of capelin, *Mallotus villosus*: an appraisal at the individual level. *Fish. Bull.* 87(3): 515–523.
- Chapman, E., Jørgensen, C., and Lutcavage, M.E. 2011. Atlantic bluefin tuna (*Thunnus thynnus*): a state-dependent energy allocation model for growth,

- maturation, and reproductive investment. *Can. J. Fish. Aquat. Sci.* **68**(11): 1934–1951. doi:10.1139/f2011-109.
- Diaz, G.A., and Turner, S.C. 2007. Size frequency distribution analysis, age composition, and maturity of western bluefin tuna in the Gulf of Mexico from the US (1981–2005) and Japanese (1975–1981) longline fleets. *Collect. Vol. Sci. Pap. ICCAT*, **60**(4): 1160–1170.
- Di Natale, A. 2017. Scientific needs for a better understanding of the Atlantic bluefin tuna (*Thunnus thynnus*) spawning areas using larval surveys. *Collect. Vol. Sci. Pap. ICCAT*, **73**(7): 2255–2279.
- Domingues, R., Goni, G., Bringas, F., Muhling, B., Lindo-Atichati, D., and Walter, J. 2016. Variability of preferred environmental conditions for Atlantic bluefin tuna (*Thunnus thynnus*) larvae in the Gulf of Mexico during 1993–2011. *Fish. Oceanogr.* **25**(3): 320–336. doi:10.1111/fog.12152.
- Fukuda, H., Torisawa, S., Sawada, Y., and Takagi, T. 2010. Ontogenetic changes in schooling behaviour during larval and early juvenile stages of Pacific bluefin tuna *Thunnus orientalis*. *J. Fish Biol.* **76**(7): 1841–1847. doi:10.1111/j.1095-8649.2010.02598.x. PMID:20557635.
- Galuardi, B., and Lutcavage, M.E. 2012. Dispersal routes and habitat utilization of juvenile Atlantic bluefin tuna, *Thunnus thynnus*, tracked with mini PSAT and archival tags. *PLoS ONE*, **7**(5): e37829. doi:10.1371/journal.pone.0037829. PMID:22629461.
- Galuardi, B., Royer, F., Golet, W., Logan, J., Neilson, J., and Lutcavage, M.E. 2010. Complex migration routes of Atlantic bluefin tuna (*Thunnus thynnus*) question current population structure paradigm. *Can. J. Fish. Aquat. Sci.* **67**(6): 966–976. doi:10.1139/F10-033.
- García, A., Cortés, D., Quintanilla, J., Ramírez, T., Quintanilla, L., Rodríguez, J.M., and Alemany, F. 2013. Climate-induced environmental conditions influencing interannual variability of Mediterranean bluefin (*Thunnus thynnus*) larval growth. *Fish. Oceanogr.* **22**(4): 273–287. doi:10.1111/fog.12021.
- Goldstein, J., Heppell, S., Cooper, A., Brault, S., and Lutcavage, M.E. 2007. Reproductive status and body condition of Atlantic bluefin tuna in the Gulf of Maine, 2000–2002. *Mar. Biol.* **151**(6): 2063–2075. doi:10.1007/s00227-007-0638-8.
- Green, B.S. 2008. Chapter 1: Maternal effects in fish populations. *Adv. Mar. Biol.* **54**: 1–105. doi:10.1016/S0065-2881(08)00001-1.
- Habtes, S., Muller-Karger, F.E., Roffer, M.A., Lamkin, J.T., and Muhling, B.A. 2014. A comparison of sampling methods for larvae of medium and large epipelagic fish species during spring SEAMAP ichthyoplankton surveys in the Gulf of Mexico. *Limnol. Oceanogr. Methods*, **12**: 86–101. doi:10.4319/lom.2014.12.86.
- Heinisch, G., Rosenfeld, H., Knapp, J.M., Gordin, H., and Lutcavage, M.E. 2015. Sexual maturity in western Atlantic bluefin tuna. *Sci. Rep.* **4**: 7205. doi:10.1038/srep07205. PMID:25431301.
- ICCAT. 2019. 2019 SCRS Report — Executive Summary. *Collect. Vol. Sci. Pap. ICCAT*, pp. 109–131.
- Ingram, G.W., Jr. 2018. Annual indices of bluefin tuna (*Thunnus thynnus*) spawning biomass in the Gulf of Mexico (1977–2016). *Collect. Vol. Sci. Pap. ICCAT*, **74**(6): 2751–2771.
- Ingram, G.W., Jr., Richards, W.J., Lamkin, J.T., and Muhling, B. 2010. Annual indices of Atlantic bluefin tuna (*Thunnus thynnus*) larvae in the Gulf of Mexico developed using delta-lognormal and multivariate models. *Aquat. Living Resour.* **23**(1): 35–47. doi:10.1051/alr/2009053.
- Irisson, J., Paris, C.B., Guigand, C., and Planes, S. 2010. Vertical distribution and ontogenetic “migration” in coral reef fish larvae. *Limnol. Oceanogr.* **55**(2): 909–919. doi:10.4319/lo.2010.55.2.0909.
- Itoh, T., Shiina, Y., Tsuji, S., Endo, F., and Tezuka, N. 2000. Otolith daily increment formation in laboratory reared larval and juvenile bluefin tuna *Thunnus thynnus*. *Fish. Sci.* **66**(5): 834–839. doi:10.1046/j.1444-2906.2000.00135.x.
- Kane, J. 2007. Zooplankton abundance trends on Georges Bank, 1977–2004. *ICES J. Mar. Sci.* **64**(5): 909–919. doi:10.1093/icesjms/fsm066.
- Kerr, L.A., Cadrin, S.X., Secor, D.H., and Taylor, N. 2013. A simulation tool to evaluate effects of mixing between Atlantic bluefin tuna stocks. *Collect. Vol. Sci. Pap. ICCAT*, **69**(2): 742–759.
- Lamkin, J.T., Muhling, B.A., Malca, E., Laiz-Carrión, R., Gerard, T., Privoznik, S., et al. 2014. Do western Atlantic bluefin tuna spawn outside of the Gulf of Mexico? Results from a larval survey in the Atlantic Ocean in 2013. *Collect. Vol. Sci. Pap. ICCAT*, **71**(4): 1736–1745.
- Lamkin, J.T., Le Hénaff, M., Smith, R., and Kourafalou, V.H. 2019. Biophysical interactions driving tuna larvae presence in Cuban waters in the Gulf of Mexico — Recent efforts by NOAA-SEFSC, NOAA-AOML and UM-RSMAS-CIMAS. In *Proceedings—The Gulf of Mexico Workshop on International Research (OCS Study BOEM 2019-045)*.
- Lindo-Atichati, D., Bringas, F., Goni, G., Muhling, B., Muller-Karger, F.E., and Habtes, S. 2012. Varying mesoscale structures influence larval fish distribution in the northern Gulf of Mexico. *Mar. Ecol. Prog. Ser.* **463**: 245–257. doi:10.3354/meps09860.
- Llopiz, J.K., and Hobday, A.J. 2015. A global comparative analysis of the feeding dynamics and environmental conditions of larval tunas, mackerels, and billfishes. *Deep-Sea Res. Part II Top. Stud. Oceanogr.* **113**: 113–124. doi:10.1016/j.dsr2.2014.05.014.
- Lutcavage, M.E., Brill, R.W., Skomal, G.B., Chase, B.C., and Howey, P.W. 1999. Results of pop-up satellite tagging of spawning size class fish in the Gulf of Maine: do North Atlantic bluefin tuna spawn in the mid-Atlantic? *Can. J. Fish. Aquat. Sci.* **56**(2): 173–177. doi:10.1139/cjfas-56-2-173.
- Malca, E., Muhling, B., Franks, J., García, A., Tilley, J., Gerard, T., et al. 2017. The first larval age and growth curve for bluefin tuna (*Thunnus thynnus*) from the Gulf of Mexico: Comparisons to the Straits of Florida, and the Balearic Sea (Mediterranean). *Fish. Res.* **190**: 24–33. doi:10.1016/j.fishres.2017.01.019.
- Mather, F.J., Mason John M.J., and Jones, A.C. 1995. Historical document: Life history and fisheries of Atlantic bluefin tuna. NOAA Technical Memorandum, NMFS-SEFSC. 405.
- McGowan, M.F., and Richards, W.J. 1989. Bluefin tuna, *Thunnus thynnus*, larvae in the Gulf Stream off the southeastern United States: satellite and shipboard observations of their environment. *Fish. Bull.* **87**(3): 615–631.
- Muhling, B.A., Lamkin, J.T., and Roffer, M.A. 2010. Predicting the occurrence of Atlantic bluefin tuna (*Thunnus thynnus*) larvae in the northern Gulf of Mexico: Building a classification model from archival data. *Fish. Oceanogr.* **19**(6): 526–539. doi:10.1111/j.1365-2419.2010.00562.x.
- Muhling, B.A., Lee, S.-K., Lamkin, J.T., and Liu, Y. 2011. Predicting the effects of climate change on bluefin tuna (*Thunnus thynnus*) spawning habitat in the Gulf of Mexico. *ICES J. Mar. Sci.* **68**(6): 1051–1062. doi:10.1093/icesjms/ fsr008.
- Muhling, B.A., Reglero, P., Ciannelli, L., Alvarez-Berastegui, D., Alemany, F., Lamkin, J.T., and Roffer, M.A. 2013. Comparison between environmental characteristics of larval bluefin tuna *Thunnus thynnus* habitat in the Gulf of Mexico and western Mediterranean Sea. *Mar. Ecol. Prog. Ser.* **486**: 257–276. doi:10.3354/meps10397.
- Muhling, B.A., Liu, Y., Lee, S.-K., Lamkin, J.T., Roffer, M.A., Muller-Karger, F., and Walter, J.F. 2015. Potential impact of climate change on the Intra-Americas Sea: Part 2. Implications for Atlantic bluefin tuna and skipjack tuna adult and larval habitats. *J. Mar. Syst.* **148**: 1–13. doi:10.1016/j.jmarsys.2015.01.010.
- Northeast Fisheries Science Center and Southeast Fisheries Science Center. 2016. Annual Report of a comprehensive assessment of marine mammal, marine turtle, and seabird abundance and spatial distribution in US waters of the western North Atlantic Ocean — AMAPPS II. *Tech. Rep.* pp. 1–53.
- Peck, M.A., Huebert, K.B., and Llopiz, J.K. 2012. Intrinsic and extrinsic factors driving match–mismatch dynamics during the early life history of marine fishes. *Adv. Ecol. Res.* **47**: 177–302. doi:10.1016/B978-0-12-398315-2.00003-X.
- Puncher, G.N., Cariani, A., Maes, G.E., Van Houdt, J., Herten, K., Cannas, R., et al. 2018. Spatial dynamics and mixing of bluefin tuna in the Atlantic Ocean and Mediterranean Sea revealed using next-generation sequencing. *Mol. Ecol. Resour.* **18**(3): 620–638. doi:10.1111/1755-0998.12764. PMID:29405659.
- Reglero, P., Blanco, E., Alemany, F., Ferrá, C., Alvarez-Berastegui, D., Ortega, A., et al. 2018a. Vertical distribution of Atlantic bluefin tuna *Thunnus thynnus* and bonito *Sarda sarda* larvae is related to temperature preference. *Mar. Ecol. Prog. Ser.* **594**: 231–243. doi:10.3354/meps12516.
- Reglero, P., Ortega, A., Balbín, R., Abascal, F.J., Medina, A., Blanco, E., et al. 2018b. Atlantic bluefin tuna spawn at suboptimal temperatures for their offspring. *Proc. R. Soc. B Biol. Sci.* **285**(1870): 20171405. doi:10.1098/rspb.2017.1405. PMID:29321292.
- Richards, W.J., and Potthoff, T. 1974. Analysis of the taxonomic characters of young scombrid fishes, genus *Thunnus*. In *The early life history of fish. Edited by J.H.S. Blaxter*. Springer, Berlin Heidelberg. pp. 623–648.
- Richardson, D.E., Marancik, K.E., Guyon, J.R., Lutcavage, M.E., Galuardi, B., Lam, C.H., et al. 2016a. Discovery of a spawning ground reveals diverse migration strategies in Atlantic bluefin tuna (*Thunnus thynnus*). *Proc. Natl. Acad. Sci. U.S.A.* **113**(12): 3299–3304. doi:10.1073/pnas.1525636113. PMID:26951668.
- Richardson, D.E., Marancik, K.E., Guyon, J.R., Lutcavage, M.E., Galuardi, B., Lam, C.H., et al. 2016b. Reply to Safina and Walter et al.: Multiple lines of evidence for size-structured spawning migrations in western Atlantic bluefin tuna. *Proc. Natl. Acad. Sci.* **113**(30): E4262–E4263. doi:10.1073/pnas.1607666113. PMID:27436889.
- Rodriguez-Ezpeleta, N., Diaz-Arce, N., Walter, J.F., Richardson, D.E., Rooker, J.R., Nottestad, L., et al. 2019. Determining natal origin for improved management of Atlantic bluefin tuna. *Front. Ecol. Environ.* **17**(8): 439–444. doi:10.1002/fee.2090.
- Rooker, J.R., Secor, D.H., de Metrio, G., Schloesser, R., Block, B.A., and Neilson, J.D. 2008. Natal homing and connectivity in Atlantic bluefin tuna populations. *Science*, **322**(5902): 742–744. doi:10.1126/science.1161473. PMID:18832611.
- Rooker, J.R., Arrizabalaga, H., Fraile, I., Secor, D.H., Dettman, D.L., Abid, N., et al. 2014. Crossing the line: migratory and homing behaviors of Atlantic bluefin tuna. *Mar. Ecol. Prog. Ser.* **504**: 265–276. doi:10.3354/meps10781.
- Rypina, I.I., Llopiz, J.K., Pratt, L.J., and Lozier, M.S. 2014. Dispersal pathways of American eel larvae from the Sargasso Sea. *Limnol. Oceanogr.* **59**(5): 1704–1714. doi:10.4319/lo.2014.59.5.1704.
- Rypina, I.I., Pratt, L.J., and Lozier, M.S. 2016. Influence of ocean circulation changes on the inter-annual variability of American eel larval dispersal. *Limnol. Oceanogr.* **61**(5): 1574–1588. doi:10.1002/lno.10297.
- Rypina, I.I., Chen, K., Hernández, C.M., Pratt, L.J., and Llopiz, J.K. 2019. Investigating the suitability of the Slope Sea for Atlantic bluefin tuna spawning using a high-resolution ocean circulation model. *ICES J. Mar. Sci.* **76**: 1666–1677. doi:10.1093/icesjms/fsz079.
- Rypina, I.I., Dotzel, M.M., Pratt, L.J., Hernandez, C.M., and Llopiz, J.K. 2021. Exploring interannual variability in potential spawning habitat for Atlantic bluefin tuna in the Slope Sea. *Prog. Oceanogr.* **192**: 102514. doi:10.1016/j.pocean.2021.102514.
- Safina, C. 2016. Data do not support new claims about bluefin tuna spawning or abundance. *Proc. Natl. Acad. Sci. U.S.A.* **113**(30): E4261–E4261. doi:10.1073/pnas.1606077113. PMID:27436891.
- Scott, G.P., Turner, S.C., Grimes, C.B., Richards, W.J., and Brothers, E.B. 1993. Indices of larval bluefin tuna, *Thunnus thynnus*, abundance in the Gulf of

- Mexico; modelling variability in growth, mortality, and gear selectivity. *Bull. Mar. Sci.* **53**(2): 912–929.
- Sponaugle, S., Llopiz, J.K., Havel, L.N., and Rankin, T.L. 2009. Spatial variation in larval growth and gut fullness in a coral reef fish. *Mar. Ecol. Prog. Ser.* **383**: 239–249. doi:[10.3354/meps07988](https://doi.org/10.3354/meps07988).
- Walsh, H.J., Richardson, D.E., Marancik, K.E., and Hare, J.A. 2015. Long-term changes in the distributions of larval and adult fish in the northeast U.S. shelf ecosystem. *PLoS ONE*, **10**(9): e0137382-31. doi:[10.1371/journal.pone.0137382](https://doi.org/10.1371/journal.pone.0137382). PMID:26398900.
- Walter, J.F., Porch, C.E., Laretta, M.V., Cass-Calay, S.L., and Brown, C.A. 2016. Implications of alternative spawning for bluefin tuna remain unclear. *Proc. Natl. Acad. Sci. U.S.A.* **113**(30): 4259–4260. doi:[10.1073/pnas.1605962113](https://doi.org/10.1073/pnas.1605962113).
- Yúfera, M., Ortiz-Delgado, J.B., Hoffman, T., Siguero, I., Urup, B., and Sarasquete, C. 2014. Organogenesis of digestive system, visual system and other structures in Atlantic bluefin tuna (*Thunnus thynnus*) larvae reared with copepods in mesocosm system. *Aquaculture*, **426–427**: 126–137. doi:[10.1016/j.aquaculture.2014.01.031](https://doi.org/10.1016/j.aquaculture.2014.01.031).